Theor Chem Account (2008) 120:543–550
DOI 10.1007/s00214-008-0439-2

REGULAR ARTICLE

On the nature of the interaction between H_2 and metal-organic frameworks

Agnieszka Kuc · Thomas Heine · Gotthard Seifert · Hélio A. Duarte

Received: 14 November 2007 / Accepted: 6 March 2008 / Published online: 26 March 2008

Abstract The mechanism of adsorption of molecular hydrogen (H_2) on IRMOF-1 is studied at the MP2 level. The role of the two principal MOF components, the inorganic connector and the organic linker, for H_2 adsorption is evaluated. Correlation methods and large basis sets are necessary to describe correctly the weak interactions (London dispersion) and to account for the polarisability of H_2. We proof that the electrostatic interactions have a negligible contribution to the interaction energy and the adsorption mechanism is governed by London dispersion (3–5 kJ mol^{-1}).

Keywords London dispersion · Electrostatic interaction · IRMOF-1 · MP2 · DFT · Hydrogen storage

1 Introduction

The onboard hydrogen storage for mobile applications has been a challenging subject over the past years. The presently available systems, high-pressure or liquefied hydrogen tanks, posses several disadvantages, among them large size, low safety and inconvenient range of pressures and temperatures for hydrogen storage. A possible solution for this problem would be to store hydrogen in low-weight solids. H_2 may be stored in solids by two principal mechanisms: chemisorption of hydrogen atoms (e.g. metal hydrides [1,2] aminoboranes [3], etc.), and physisorption of hydrogen molecules in nanoporous, e.g. carbon-based, materials [4–6]. As H_2 is a neutral molecule with a small polarizability, the two main contributions to the adsorption energy are weak London (dispersion) interactions and electrostatic interactions with dipole at H_2 induced by the polarity of the host system. The dispersion interaction depends on the polarizability of H_2 and of the host material, and on the distance between them. Good storage media should have high polarizability and a large surface area with a pore size of ∼0.6 nm [6–8]. The class of light, highly porous carbon materials belongs to this group, and hydrogen storage capacities have already been discussed for graphitic (sp^2) carbon structures [graphene slit pores [8], carbon nanotubes [9], fullerenes [10] and more advanced materials (C_{60} intercalated graphite [11], honeycomb graphite [12,13], etc.)]. However, their systematic engineering and identification of specific adsorption sites is difficult. So far, the highest reliable storage capacity was observed for superactivated carbon [14].

Thus, the goal of the US Department of Energy (6 wt% of stored H_2 and 45 g L^{-1} volumetric density [15]) was not yet reached with any of the investigated materials for moderate pressures and ambient temperature [16,17]. Efficient H_2 storage could be improved by introduction of attractive electrostatic interactions. The host material should, therefore, have a strong surface polarization which can polarize adsorbed H_2 molecules and increase the guest–host interaction.

Among the family of highly porous materials, metal-organic frameworks (MOFs, see Fig. 1a) [18,19], have recently been proposed as one of the most promising materials

Dedicated to the 60th birthday of Prof. Nino Russo.

A. Kuc · T. Heine · G. Seifert
Physikalische Chemie, Technische Universität Dresden,
01062 Dresden, Germany

T. Heine (✉)
School of Engineering and Sciences, Jacobs University Bremen,
28759 Bremen, Germany
e-mail: t.heine@jacobs-university.de

H. A. Duarte
Grupo de Pesquisa em Química Inorgânica Teórica,
Departamento de Química, ICEx, Universidade Federal
de Minas Gerais, Belo Horizonte,
MG 31.270-901, Brazil

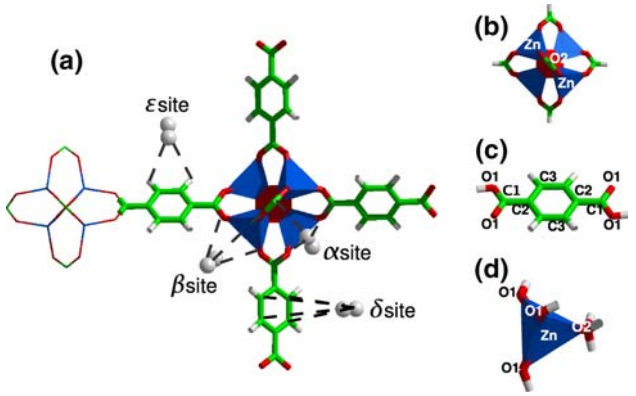

Fig. 1 The considered adsorption sites within the IRMOF-1 unit cell **a** and the used model systems: **b** the connector, $Zn_4O(HCO_2)_6$, **c** the linker, $C_6H_4(COOH)_2$ and **d** the alternative connector model, ZnO_4H_6. The atom numbering is shown, as well

with these properties. They are built of predefined building blocks, metal oxide centers (connectors) and organic linkers based on aromatic carbon connections. The architecture, functionalization and the pore size distribution of MOFs are possible to control. Thus, many applications for these systems have been proposed, among them H_2 storage [20–22].

The fundamental interactions underlying the H_2 adsorption in MOFs have to be well understood in order to tune the storage capacity of these materials. So far, it is not clear which interaction (London dispersion or electrostatics) is mainly responsible for the H_2 physisorption in MOFs. Experimental investigations suggest that the strongest H_2 adsorption sites are close to the metal oxide connectors [22]. This is interpreted such that metal cations form M–O (M=Zn, Cu, Mg, etc.) dipoles whose charges are most effective in polarizing the gas molecules, leading to strong interactions. On the other hand, theoretical investigations discuss this interpretation rather controversially: while several authors agree that the interaction of H_2 with the organic linkers is pure London dispersion with interaction energies of 3.5–5 kJ mol^{-1} [23–25], the values reported for the interaction with the zinc oxide connector of IRMOF-1 vary much stronger, between 2 and 7 kJ mol^{-1} [24–29]. More importantly, different origins of the interaction have been suggested, namely dipole–induced dipole interactions [29] and weak London dispersion [26]. We have recently shown that the electrostatic contribution is negligible, and the H_2–MOF interaction is based almost exclusively on London dispersion [30].

Low-energy adsorption sites of H_2 in MOFs have been identified already, for example using DFT calculations in extended systems [24,27,31,32], whose results are in qualitative agreement with experiment [22,32]. The corresponding interaction energies lack, however, correct treatment of London dispersion, and are therefore not reliable. The aim of this work is to contribute to a better understanding of the fundamental interactions of H_2 with MOFs, and to deepen the discussion of our earlier findings on the basis of high-level quantum chemical calculations. A major problem to be solved is to attribute the nature of H_2–MOF interactions to London dispersion and to electrostatic interactions. The results of these calculations should provide sufficient data to establish a dispersion-corrected DFT treatment in the spirit of Grimme's or von Lilienfeld's approaches [33,34], which has the power to become the method of choice for treatment of host–guest interactions in MOFs. We have chosen the most widely investigated IRMOF-1 as a benchmark system. While a brief introduction to this work was already presented in our previous communication [30], this article covers a wide range of detailed high-level calculations in order to determine the accurate treatment of weakly bound H_2 in MOFs.

2 Models and methods

The accurate calculation of the interaction of H_2 with MOFs needs the representation of the extended system (Fig. 1a) as smaller model structures. The models we have studied for the IRMOF-1 are shown in Fig. 1b, c. The $Zn_4O(HCO_2)_6$ cluster (Fig. 1b) was used to model the connector and benzene-1,4-dicarboxylate, $C_6H_4(COOH)_2$ (Fig. 1c) for the linker. The connector can be viewed as tetrahedral arrangement of Zn atoms around the central O atom and four distorted tetrahedral of ZnO_4 moieties. The high-symmetry adsorption sites, proposed from neutron scattering experiments [22], are also indicated in Fig. 1a.

It is well-known that London dispersion, which gives an important contribution to the physisorption energy of weakly bound systems, is a correlation phenomenon, and therefore not included in the Hartree–Fock (HF) method. HF does account, however, correctly for electrostatic interactions (charge–dipole, dipole–dipole, dipole–induced dipole) and Pauli repulsion. The long-range interaction is also poorly described in the presently available exchange-correlation functionals in Density Functional Theory [35]. Our results (see Tables 1, 2) show that for the gradient-corrected hybrid functional PBE0 [36], the distances between the molecular centers are close to the equilibrium, however, the interaction energies are far from the correct values. The long-range interaction is, however, correctly included in the post-Hartree–Fock methods that properly treat correlation effects. The second order Møller–Plesset (MP2) perturbation theory is a method which is feasible to treat the systems discussed in this article, even with larger basis sets, and still providing sufficient accuracy. As we will see below, a high accuracy can only be achieved if the interaction energies are corrected for basis set superposition errors (BSSE) [37].

The model structures have been optimized at the B3LYP/6-31G(d) level using the Gaussian03 [38–41] code. The

Table 1 δ site of the linker

Method/basis set	No BSSE		BSSE	
	E [kJ/mol]	d [Å]	E [kJ/mol]	d [Å]
Model I				
PBE/cc-pvTZ	1.30	3.3	1.27	3.3
MP2/cc-pvDZ	3.50	3.2	1.70	3.4
MP2/cc-pvTZ	4.61	3.1	3.44	3.2
Model II				
PBE/cc-pvTZ	0.79	3.45	0.68	3.45
MP2/cc-pvDZ	1.76	3.2	0.65	3.5
MP2/cc-pvTZ	3.46	3.0	2.64	3.1
Model III				
PBE/cc-pvTZ	0.98	3.4	0.83	3.4
MP2/cc-pvDZ	1.94	3.2	0.73	3.4
MP2/cc-pvTZ	3.73	3.0	2.87	3.1

Table 2 Smaller model connectors, β site

Method/basis set	No BSSE		BSSE	
	E [kJ/mol]	d [Å]	E [kJ/mol]	d [Å]
Model BI				
PBE/cc-pvTZ/6-31+G(2d,p)	3.74	3.8	2.25	4.0
cc-pvDZ-PP	4.29	3.1	2.19	4.1
cc-pvTZ-PP	6.25	3.1	2.35	4.0
cc-pvQZ-PP	5.32	3.1	2.46	3.9
aug-cc-pvDZ-PP	7.35	3.4	2.26	4.0
aug-cc-pvDZ/6-31+G(2d,p)	4.37	3.7	2.23	4.0
aug-cc-pvTZ-PP	5.11	3.6	2.45	3.9
aug-cc-pvTZ/6-31+G(2d,p)	7.33	3.2	2.40	3.9
aug-cc-pvQZ/6-31+G(2d,p)	8.95	3.2	2.46	3.9
Model BII				
PBE/cc-pvTZ/6-31+G(2d,p)	5.52	2.9	2.22	3.0
cc-pvDZ-PP	8.02	2.8	0.22	3.6
cc-pvTZ-PP	7.87	2.8	2.32	3.1
aug-cc-pvDZ-PP	10.14	2.8	2.85	3.1
aug-cc-pvDZ/6-31+G(2d,p)	6.76	2.9	2.92	3.1
aug-cc-pvTZ-PP	5.99	2.8	3.95	2.9
aug-cc-pvTZ/6-31+G(2d,p)	8.65	2.7	3.85	3.0
aug-cc-pvQZ-PP	5.57	2.8	4.33	2.9
aug-cc-pvQZ/6-31+G(2d,p)	10.77	2.6	4.17	2.9

(All values are MP2 calculations if not indicated explicitly)

fragments have been kept fixed for the calculations of interaction energies between H_2 and the models of the MOFs. Various high-level calculations available in the literature [7, 42,43] agree that MP2 theory with moderately large basis sets can describe the weak interactions between a hydrogen molecule and systems similar to the nonpolar linker with sufficient accuracy. Figures 2a and 3a demonstrate that these findings apply also for MOF linkers (see also Table 1). They can be treated with good accuracy at the MP2/cc-pvTZ level with BSSE correction.

However, the H_2 interaction with inorganic connectors was less precisely studied in the literature. The connector model, shown in Fig. 1b, has too many electrons for a high-level calculation. Therefore we have chosen a smaller model, ZnO_4H_6 (Fig. 1d), to benchmark the level of theory. This model can describe the physisorption of H_2, only at the β adsorption site. The basis set dependence of the MP2 results of the H_2 interaction with the ZnO_4H_6 model (Fig. 4, BI) is shown in Fig. 2b, c. The corresponding results for other H_2 orientation (Fig. 4, BII) are presented in Fig. 3b, c. The fast convergence of the BSSE corrected interaction energies to a maximum value of 2.5 and 4.2 kJ mol^{-1} has been obtained, for the model BI and BII, respectively. On the other hand, the BSSE uncorrected numbers strongly overestimate interaction energies, with values which can be as large as 10 kJ mol^{-1}. It is well known that combined large and moderate basis sets can give meaningless results. The long-ranged polarization and diffuse functions increase the basis set on the host to accommodate its electrons and results in a significantly lowered energy for the H_2–host system. Systematic investigations on the basis set size showed that for the aug-cc-pvTZ basis set [44] for C, O and H and aug-cc-pVTZ-PP for Zn the BSSE corrected interaction energies are in close agreement with the converged results (see Table 2), underestimated by only 0.2 kJ mol^{-1}.

To study the H_2 interaction with our connector model this level of theory is still too expensive. Therefore we reduced the basis set for atoms far from the interaction site to 6-31+G(2d,p) or even to 6-31G(d) bases. However, it is necessary to keep the large basis on H_2 and its closest neighbors to allow a high-level description of the weak interaction between the two moieties. While the BSSE uncorrected results are meaningless for weakly bound systems, our BSSE corrected results are close to those of converged MP2 calculations with balanced basis sets (see Table 2). Therefore, this computational strategy can be safely adopted in the remainder of this and future work.

Considering the electrostatic effects, the strongest polarization of H_2 can be expected if the hydrogen molecule is oriented along the axis of the central Zn–O bond of the connector (see Fig. 4 BI). Figure 2d shows the H_2–connector interaction results for BI at the basis-set converged HF level of theory. If we assume that the total interaction (the MP2 result) is only London dispersion and electrostatic interaction, the HF result should account for the latter one, as London dispersion is not included here. Indeed, with this assumption electrostatics accounts for about 50% of the total interaction energy in this orientation. However, results for the perpendicular orientation (see Fig. 4 BII) indicate no electrostatic interactions, as the interaction energy at the HF level is negligible (see Fig. 3d). It is worth to point out that the total

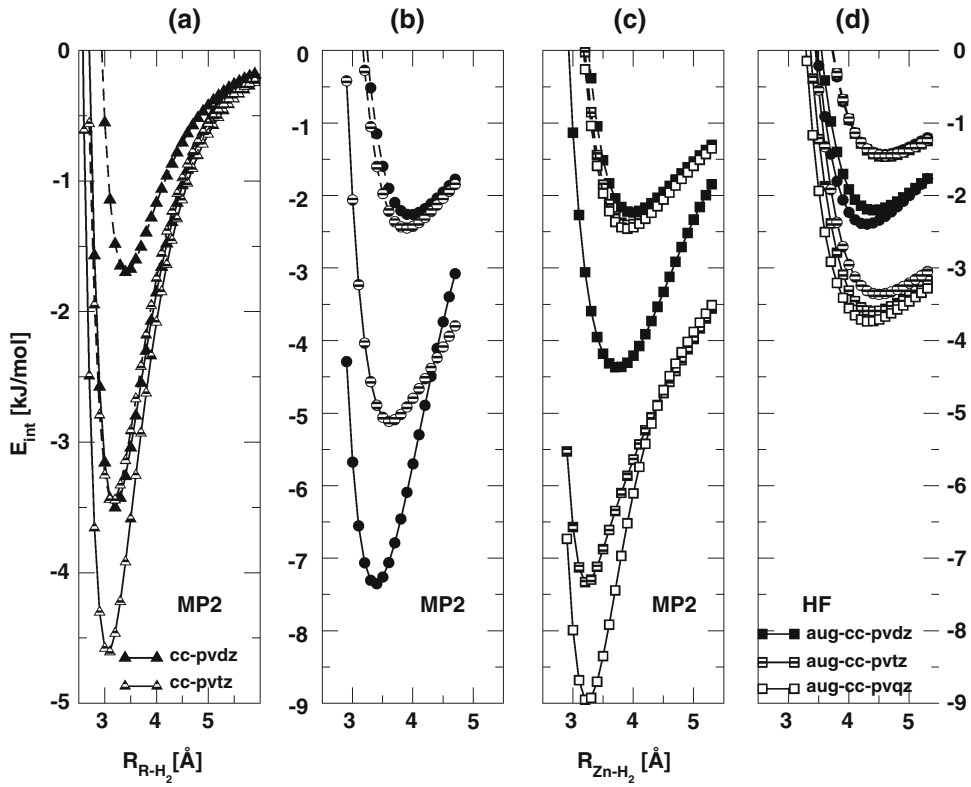

Fig. 2 The potential energy curves of H_2 to the linker (model I, see Fig. 4) and connector (model BI) at MP2 **a**–**c** and HF **d** levels. *Solid lines* give the relative energy of the adsorbed with respect to the dissociated systems. *Dashed lines* denote those results corrected for basis set superposition errors. Basis sets are given in the plots, **c** shows results where small basis sets [6–31 + G(2d,p)] have been employed at positions far from the adsorption site (see text)

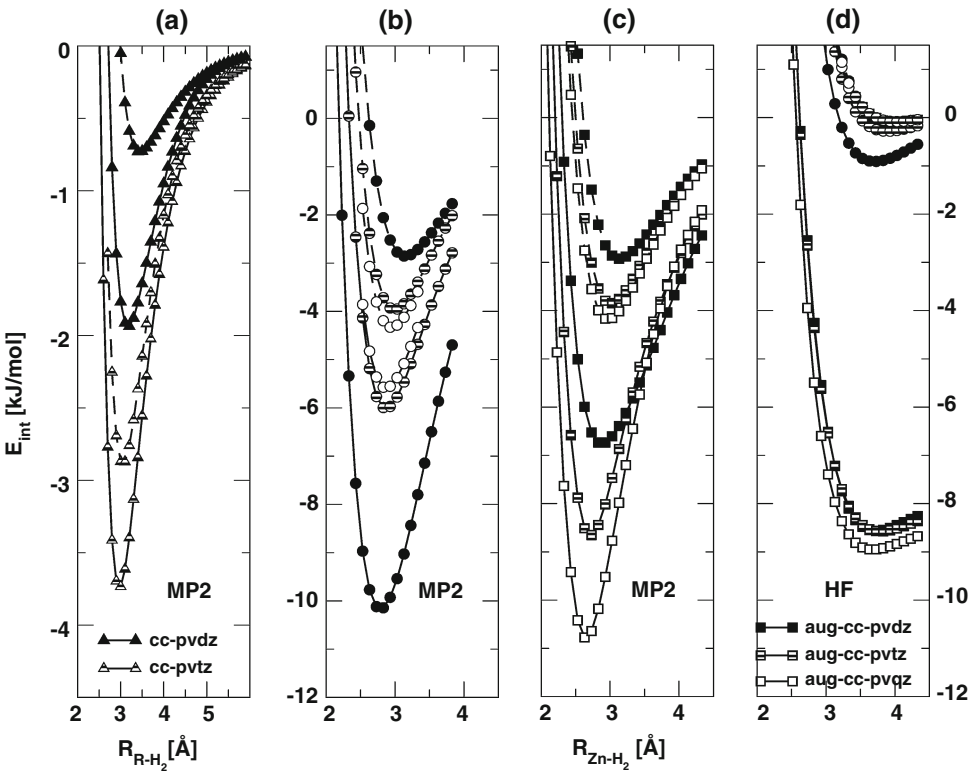

Fig. 3 The potential energy curves of H_2 to the linker (model III, see Fig. 4) and connector (model BII) at MP2 **a**–**c** and HF **d** levels. *Solid lines* give the relative energy of the adsorbed with respect to the dissociated systems. *Dashed lines* denote those results corrected for basis set superposition errors. Basis sets are given in the plots, **c** small basis sets [6–31 + G(2d,p)] have been employed at positions far from the adsorption site (see text)

interaction energy (MP2 results) is stronger for BII than for BI, even though it is based almost exclusively on London dispersion. The overestimated interaction energy (HF level) without counterpoise corrections (independent on the H_2 orientation) is an artifact of the finite basis set, but not related to any physical interaction.

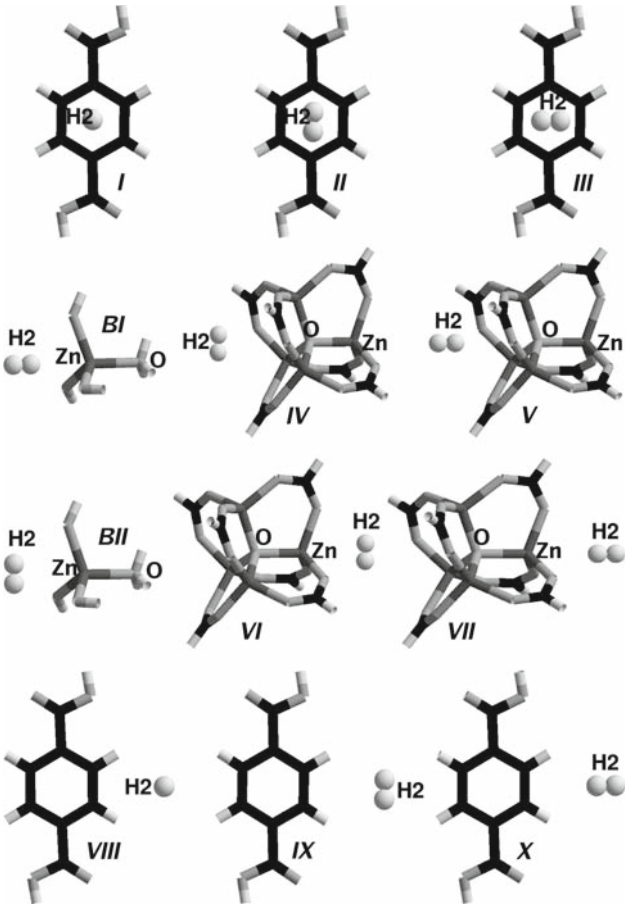

Fig. 4 Model structures and H_2 orientations: I–III and VII–X for the linker, IV–VII for the larger connector and BI–BII for the benchmark connector

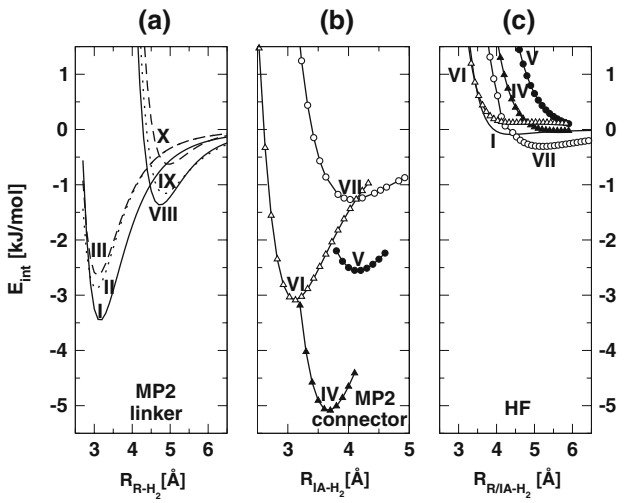

Fig. 5 The interaction of H_2 with IRMOF-1 linker **a** and connector **b** as function of the H_2–host distance. In **c** the electrostatic contribution to the interaction from HF calculations is shown. Model structures and adsorption sites are given in Fig. 3

Our benchmark calculations show that the H_2–connector interaction energy can be calculated correctly at the MP2 level with aug-cc-pvTZ basis sets at the H_2 molecule and its closest neighbors, and a small basis (6-31G(d)) for the remaining cluster. However, the BSSE corrections have to be applied. The interaction between the hydrogen molecule and the linker can be treated accurately already at the MP2/cc-pvTZ level including the counterpoise correction. Smaller basis sets are not appropriate for this class of weakly bound systems (see Tables 1,2). The difference between MP2 and HF interaction energies can be attributed to London dispersion interaction. In the following we discuss the H_2 adsorption on high-symmetry sites of IRMOF-1 using the $Zn_4O(HCO_2)_6$ model system.

3 Results and discussion

Figure 5 shows the interaction energy between H_2 and various adsorption site models of IRMOF-1 (I to X from Fig. 4) for a range of distances between both species. For the δ adsorption site (Fig. 4, I), where H_2 points to the ring center of the linker in perpendicular orientation, the highest interaction energy of 3.44 kJ mol^{-1} (Fig. 5a) is very similar to that of H_2 with benzene (3.78 kJ mol^{-1}) [43]. Our result is close to that of Buda et al. [23] (3.18 kJ mol^{-1} RI-MP2/cc-pvTZ). The equilibrium distance was found to be 3.2 Å. When H_2 is oriented parallel to the ring (models II and III), the interaction is 1 kJ mol^{-1} weaker, but the distance between the molecular centers is about the same. Both parallel orientations are energetically equivalent to each other. The presence of hydroxyl groups does not change significantly the strength of physisorption. We do not find any attraction at the HF level (Fig. 5c) for the δ site and so we attribute this interaction exclusively to London dispersion.

Moreover, there is an alternative organic linker site (Fig. 4 VIII–X), the so-called, ε site. Here the interaction energy is significantly lower, 1.4 kJ mol^{-1} (see Table 3) than at the corresponding δ site. This result is in good agreement with the results of Buda et al. [23], who found the interaction energy on ε site of 1.26 kJ mol^{-1}. However, as many of these sites are present in IRMOF-1 and London dispersion interactions are additive they probably contribute also to the high H_2 adsorption capacities reported in the experiment [20–22,45]. The distances between molecular centers for this adsorption site are about 1.5 Å longer than those for the δ site. Both parallel orientations are not equivalent (see Fig. 5a) and the interaction with H_2 is very weak: 1.16 and 0.63 kJ mol^{-1}.

For the connector model (Fig. 1b) the interaction mechanism is different (Fig. 5b). Although in the adsorption β site, models VI and VII (Fig. 4), the Zn atom is well exposed to the H_2 molecule, the lack of other atoms surrounding the H_2 prevents larger dispersion energy contributions to the

Table 3 ε site of the linker: MP2/cc-pVTZ level

No BSSE		BSSE	
E [kJ/mol]	d [Å]	E [kJ/mol]	d [Å]
Model VIII			
1.70	4.7	1.36	4.7
Model IX			
1.43	4.8	1.16	4.8
Model X			
1.00	4.9	0.63	5.0

Table 4 Big model: α and β site with both H_2 orientations

	Perpendicular 1		Parallel	
Adsorption site	E [kJ/mol]	d [Å]	E [kJ/mol]	d [Å]
α	5.09	3.7	2.55	4.2
β	3.09	3.1	1.27	4.0

(The distances are given between the molecular center of H_2 and the central O atom (on α site) and the closest Zn atom (on β site). BSSE corrected number are given)

Table 5 Big model: both H_2 perpendicular orientations, no BSSE

	Perpendicular 1		Perpendicular 2	
Adsorption site	E [kJ/mol]	d [Å]	E [kJ/mol]	d [Å]
β	3.53	3.1	3.53	3.1
α	10.26	3.3	10.28	3.3

binding energy. The strongest interaction is found when H_2 is perpendicular to the central Zn–O bond (VI). The equilibrium distance between the center of H_2 and the closest interaction atom (Zn atom) is 3.1 Å and the interaction energy is 3.1 kJ mol^{-1} (see Table 4), which is 0.3 kJ mol^{-1} less than for the linker. Bordiga et al. [26] found, however, the interaction energy of 1 kJ mol^{-1} smaller than our findings, while their reported equilibrium distance is about the same (3.18 Å). Even smaller interaction energy (1.34 kJ mol^{-1}) was found for this site by Klontzas et al. [29] at the IR-MP2/TZVPP level. As the interaction is independent on the azimuthal orientation of H_2 to the Zn–O axis (see Table 5) we have studied in detail only one perpendicular orientation.

A much weaker interaction of only 1.3 kJ mol^{-1} was found for the parallel orientation of H_2 to the central Zn–O bond (model VII). The equilibrium distance of 4.0 Å from Zn atom is more than 1 Å longer than for the perpendicular orientation. These findings are close to the results of Klontzes et al. [29], who reported an interaction energy of 1.05 kJ mol^{-1} at 3.7 Å. It is important to notice that when rotating H_2 at its minimum in complex VI by 90° complex VII is obtained, with a repulsive H_2–host interaction at that position of H_2. This does not allow a stable configuration of the complex for rotating H_2. Comparing the benchmark calculations with those for the models VI and VII, our results show that the larger clusters interact less. For model VI (3.1 kJ mol^{-1}) compared to BII (3.6 kJ mol^{-1}), where the interaction is mainly London dispersion, the difference is small and the binding energy is reduced by only 0.5 kJ mol^{-1}. However, comparing VII (1.27 kJ mol^{-1}) with its smaller model BI (2.52 kJ mol^{-1}), the interaction is reduced to 50%. The distances between the molecular centers stay unchanged for both models and corresponding orientations. The difference in the interaction energy, when going from the model BI to VII, we attributed to electrostatics. The HF calculations (see Fig. 5c) indicate that there is no H_2–connector attraction. Obviously, the electrostatic interaction is significantly lower than in the smaller cluster.

Employing the Mulliken and natural bond orbital (NBO) charge analysis we have estimated the dipole moment induced on H_2, using the point charge approximation. We have considered the cases where the hydrogen molecule is physisorbed at the clusters BI and VII. The results were compared with the dipole moment of a strongly polarized H_2 molecule between two point charges of opposite signs, $q^+ - H_2 - q^-$. The point charges were placed on opposite sites of hydrogen axis at distances of 3.5 Å from the H_2 center. For the $q^+ - H_2 - q^-$ model the induced dipole moment at H_2 is 1.56 Debye using Mulliken charges. This value drops down to 0.20 (0.12 in NBO model) Debye for the BI model and almost vanishes (0.04 (0.02) Debye) for the larger adsorption model VII. We can conclude that in the connector there are no specific polarizing centers. This is also in agreement with the results of Bordiga et al. [26] and Civalleri et al. [46].

Finally, we can consider the α adsorption site where H_2 is enclosed in a sort of a pocket of three surrounding Zn atoms and carboxyl groups (see Fig. 4, IV and V). At this site there are more atoms interacting with the hydrogen molecule. This increases the contribution of the dispersive forces to the total binding energy. In model IV, H_2 fits very well into the pocket, with various interatomic distances of 3.0–3.7 Å between H atoms and their surrounding heavier atoms. Consequently we find the strongest interaction energy for this site, 5.1 kJ mol^{-1}. This result is much smaller than that of Sagara et al. [25], who reported 9.15 (without BSSE) and 6.86 kJ mol^{-1} (at the "basis set limit"). On the other hand, the experimental estimation of Bordiga et al. [26] (3.5 kJ mol^{-1}) is by 1.5 kJ mol^{-1} smaller than our findings. Similar results (3.1 kJ mol^{-1}) are reported in the work of Klontzes et al. [29]. The interaction energy is lowered significantly for this binding site if the orientation of H_2 is changed (model V). Now only one H-atom has many close contacts to the host structure. For this site (model V) we estimate only 2.5 kJ mol^{-1} at the equilibrium distance of 4.2 Å between the center of H_2 and the central O atom. This result is again larger by around 1 kJ mol^{-1} than that of [29]. Comparing the distances between the center of H_2 and "interaction atom" for the model

IV and VI, we find larger values for the α site. This can be explained again by the geometry of the connector, which permits that many neighboring atoms attract the H_2 guest molecule.

4 Conclusions

Our calculations show that the physisorption of H_2 in MOFs is mainly due to the weak London interaction between linkers and connectors with hydrogen. The small charge separation in the MOF can not induce significant dipole moment in H_2 and thus, electrostatic interactions play a minor role.

We pointed out that the correct treatment of correlation effects and application of BSSE corrections are essential for the correct estimation of H_2–MOF interaction potentials. For our connector and linker models we find similar interaction energies with molecular hydrogen. Our theoretical results qualitatively agree with experiment [22,32]: the strongest interaction is found for site α, with the sequence $\alpha > \beta > \delta \gg \varepsilon$. The most favorable orientation of hydrogen is the perpendicular orientation to the benzene ring or to the central Zn–O bond for the linker and the connector, respectively. However, H_2 can rotate nearly freely and therefore appears as a physisorbed sphere rather than a linear molecule, and mean interaction energy cannot be compared only with the most stable orientation of hydrogen molecule but has to be averaged over all orientations.

In solid MOFs the always attractive long-range interaction potentials of the nanopores will overlap and superpose to considerable values, hence a stronger interaction with H_2 is expected. The nanoporosity of MOFs can be tuned in order to maximize the interaction with H_2. We are working on a parameterization of the H_2–MOFs interaction potential which will allow detailed calculations to estimate the free interaction energy and the amount of hydrogen uptake using quantum liquid density-functional theory [17].

Acknowledgments The authors acknowledge financial support by Stiftung Energieforschung Baden-Württemberg, Deutscher Akademischer Austauschdienst (DAAD), Germany, and Coordenação de Aperfeiçoamento de Pessoal de Nível Superior (CAPES), Brazil. Authors also thank Dr. A. Jaron-Becker, Dr. L. Zhechkov, Dr. A. F. Oliveira, Dr. H. de Abreu and Dr. A. Enyashin for stimulating discussions and K. Vietze for computational assistance. Computations have been partially carried out at ZIH Dresden. Figures of structures were made using GTK Display Interface for Structures 0.86.0 program.

References

1. Schlapbach L, Zuttel A (2001) Nature 414:353
2. Perng TP, Wu JK (2003) Mater Lett 57:3437
3. Yoon CW, Sneddon LG (2006) J Am Chem Soc 128:13992
4. Chen P, Wu X, Lin J, Tan KL (2006) Science 285:91
5. Dillon AC, Jones KM, Bekkedahl TA, Kiang CH, Bethune DS, Heben MJ (1997) Nature 386:377
6. Gogotsi Y, Dash RK, Yushin G, Yildirim T, Laudisio G, Fischer JE (2005) J Am Chem Soc 127:16006
7. Patchkovskii S, Tse JS, Yurchenko SN, Zhechkov L, Heine T, Seifert G (2005) Proc Natl Acad Sci USA 102:10439
8. Wang QY, Johnson JK (1999) J Chem Phys 110:577
9. Sudan P, Zuttel A, Mauron P, Emmenegger C, Wenger P, Schlapbach L (2003) Carbon 41:2377
10. Turnbull JD, Boninsegni M (2005) Phys Rev B 71:205421-1
11. Kuc A, Zhechkov L, Patchkovskii S, Seifert G, Heine T (2007) Nano Lett 7:1
12. Karfunkel HR, Dressler T (1992) J Am Chem Soc 114:2285
13. Kuc A, Seifert G (2006) Phys Rev B 74:214104
14. Panella B, Hirscher M, Roth S (2005) Carbon 43:2209
15. http://www1.eere.energy.gov/hydrogenandfuelcells/storage
16. Kowalczyk P, Holyst R, Terrones M, Terrones H (2007) Phys Chem Chem Phys 9:1786
17. Patchkovskii S, Heine T (2007) Phys Chem Chem Phys 9:2697
18. Yaghi OM, O'Keeffe M, Ockwig NW, Chae HK, Eddaoudi M, Kim J (2003) Nature 423:705
19. Schlichte K, Kratzke T, Kaskel S (2004) Microporous Mesoporous Mater 73:81
20. Panella B, Hirscher M (2005) Adv Mater 17:538
21. Rosi NL, Eckert J, Eddaoudi M, Vodak DT, Kim J, O'Keeffe M, Yaghi OM (2003) Science 300:1127
22. Rowsell JLC, Eckert J, Yaghi OM (2005) J Am Chem Soc 127:14904
23. Buda C, Dunietz BD (2006) J Phys Chem B 110:10479
24. Mueller T, Ceder G (2005) J Phys Chem B 109:17974
25. Sagara T, Klassen J, Ganz E (2004) J Chem Phys 121:12543
26. Bordiga S, Vitillo JG, Ricchiardi G, Regli L, Cocina D, Zecchina A, Arstad B, Bjorgen M, Hafizovic J, Lillerud KP (2005) J Phys Chem B 109:18237
27. Samanta A, Furuta T, Li J (2006) J Chem Phys 125
28. Lee TB, Kim D, Jung DH, Choi SB, Yoon JH, Kim J, Choi K, Choi SH (2007) Catal Today 120:330
29. Klontzas E, Mavrandonakis A, Froudakis GE, Carissan Y, Kopper W (2007) J Phys Chem C 111:13635
30. Kuc A, Heine T, Seifert G, Duarte HA (2008) Angew Chem Int Ed (submitted)
31. Mulder FM, Dingemans TJ, Wagemaker M, Kearley GJ (2005) Chem Phys 317:113
32. Yildirim T, Hartman MR (2005) Phys Rev Let 95:215504-1
33. Grimme S (2006) J Comput Chem 27:1787
34. von Lilienfeld OA, Tavernelli I, Rothlisberger U, Sebastiani D (2004) Phys Rev Let 93
35. Zhechkov L, Heine T, Patchkovskii S, Seifert G, Duarte HA (2005) J Chem Theory Comput 1:841
36. Perdew JP, Burke K, Ernzerhof M (1996) Phys Rev Lett 77:3865
37. Boys SF, Bernardi F (1970) Mol Phys 19:553
38. Becke AD (1993) J Chem Phys 98:5648
39. Ditchfield R, Hehre WJ, Pople JA (1971) J Chem Phys 54:724
40. Frisch MJT, Schlegel GW, Scuseria HB, Robb GE, Cheeseman MA, Montgomery JR Jr., Vreven JA, Kudin T, Burant KN, Millam JC, Iyengar JM, Tomasi SS, Barone J, Mennucci V, Cossi B, Scalmani M, Rega G, Petersson N, Nakatsuji GA, Hada H, Ehara M, Toyota M, Fukuda K, Hasegawa R, Ishida J, Nakajima M, Honda T, Kitao Y, Nakai O, Klene H, Li M, Knox X, Hratchian JE, Cross HP, Bakken JB, Adamo V, Jaramillo C, Gomperts J, Stratmann R, Yazyev RE, Austin O, Cammi AJ, Pomelli R, Ochterski C, Ayala JW, Morokuma PY, Voth K, Salvador GA, Dannenberg P, Zakrzewski JJ, Dapprich VG, Daniels S, Strain D, Farkas MC, Malick O, Rabuck DK, Raghavachari AD, Foresman K, Ortiz JB, Cui JV, Baboul Q, Clifford AG, Cioslowski S, Stefanov J, Liu BB, Liashenko G, Piskorz A, Komaromi P, Martin I, Fox RL, Keith DJ,

Al-Laham T, Peng MA, Nanayakkara CY, Challacombe A, Gill M, Johnson PMW, Chen B, Wong W, Gonzalez MW, C., Pople JA (2004) Gaussian 03. Revision C.02 (Wallingford CT)
41. Lee CT, Yang WT, Parr RG (1988) Phys Rev B 37:785
42. Ferre-Vilaplana A (2005) J Chem Phys 122:104709
43. Heine T, Zhechkov L, Seifert G (2004) Phys Chem Chem Phys 6:980
44. Kendall RA, Dunning TH, Harrison RJ (1992) J Chem Phys 96:6796
45. Rowsell JLC, Yaghi OM (2005) Angew Chem Int Ed 44:4670
46. Civalleri B, Napoli F, Noel Y, Roetti C, Dovesi R (2006) Crystengcomm 8:364